Geophys. J. R. astr. Soc. (1985) **82**, 57–80

Multiple scattering and energy transfer of seismic waves – separation of scattering effect from intrinsic attenuation – I. Theoretical modelling

Ru-Shan Wu* *Earth Resources Laboratory, Department of Earth, Atmospheric, and Planetary Sciences, Massachusetts Institute for Technology, Cambridge, MA 02139, USA*

Accepted 1984 December 17. Received 1984 December 17; in original form 1984 October 4

Summary. In order to separate the scattering effect from the intrinsic attenuation, we need a multiple scattering model for seismic wave propagation in random heterogeneous media. In this paper, we apply radiative transfer theory to seismic wave propagation and formulate in the frequency domain the energy density distribution in space for a point source. We consider the cases of isotropic scattering and strong forward scattering. Some numerical examples are shown. It is seen that the energy density–distance curves have quite different shapes depending on the values of medium seismic albedo $B_0 = \eta_s/(\eta_s + \eta_a)$, where η_s is the scattering coefficient and η_a is the absorption coefficient of the medium. For a high albedo ($B > 0.5$) medium, the energy–distance curve is of arch shape and the position of the peak is a function of the extinction coefficient of the medium $\eta_e = \eta_s + \eta_a$. Therefore it is possible to separate the scattering effect and the absorption based on the measured energy density distribution curves.

1 Introduction

Are the measured apparent attenuations for short-period seismic waves caused by anelasticity of the media or by scattering of the heterogeneities in the media? Is the single backscattering model a good approximation to the coda envelope decay or do we need a multiple scattering model which will have significant differences in describing the coda behaviour from the single backscattering theory? These are long-standing problems. In order to answer these questions, we need to develop a multiple scattering model for seismic waves and compare the predictions from it with those obtained from the single scattering theory. O'Doherty & Anstey (1971) derived a one-dimensional multiple scattering formula for a stack of thin layers as

$$|T(\omega)| = \exp[-R(\omega)t], \tag{1.1}$$

*Permanent address, Institute of Geophysical and Geochemical Prospecting, Baiwanzhuang, Peking, China.

where ω is the angular frequency of the wave, $t = N\tau$ is the travel time of passing through the stack, τ is the travel time for each layer and N is the number of the layers; $T(\omega)$ is the transmission response and $R(\omega)$ is the power spectrum of the reflection coefficient series normalized by the travel time. The exponential form of (1.1) itself exhibits the indiscriminability of the multiple scattering effect from the intrinsic absorption, if we observe only the decay of the transmitted waves. Richards & Menke (1983) did some numerical experiments on this model and discussed some possibilities of using the relation between amplitude spectra, the frequency contents of the coda and that of the main arrival etc. to distinguish the multiple scattering effects of thin layers from the intrinsic attenuation. We note that the formulation of the problem by O'Doherty & Anstey is essentially that of the random slab problem (see Kay & Silverman 1958; Hoffman 1964). The results are presented as the relations of transmitted or reflected waves with the slab thickness, which do not necessarily represent the amplitude attenuation with distance or the envelope decay with time of seismic waves.

Kopnichev (1977) formulated the double and triple scattering for 2-D and 3-D media in the case of isotropic scattering. Gao *et al.* (1983a,b) derived up to seventh-order scattering and then obtained the approximate formulae of multiple scattering in time domain for 2-D and 3-D media using a curve-fitting technique. However, the formulae derived are for the case in which the source and sensor are located in the same point. On the other hand, the most prominent evidence of multiple scattering would be manifested if the sensor could be situated at some place between the source and the point apart from the source by one mean free path of scattering (this will be shown later). Therefore it may be difficult to use these formulae for discriminating the scattering attenuation from the intrinsic attenuation, though the formulation may be very useful in other calculations.

In this paper, we derive the formulation of seismic energy transfer under multiple scattering by using the radiative transfer equation technique developed in the astrophysical optics and the neutron transport theory and explore the possibilities of using this approach to separate the scattering and intrinsic attenuation.

Historically, multiple scattering theory has been developed along two independent approaches: the analytic theory and the transport theory (for review see Ishimaru 1977). Both are based on the statistical treatment of wave propagation in random media. Because the complex heterogeneities are modelled with a random medium, the wavefields propagating therein are also random wavefields. We are interested only in some statistical quantities of the wavefield, such as the mean intensity, phase and amplitude fluctuations, various correlation functions, pulse spreading, angular broadening, etc. All of these quantities can be obtained from the moments of the random field. The analytic theory starts with basic differential equations such as wave equations and, by introducing the scattering and absorption characteristics of the random heterogeneities, derives the differential or integro-differential equations for the moments of the wavefields. There are basically two branches in the analytic theory: the renormalization method and the small-angle approximation method. In the first branch the renormalization procedure was used for the formal perturbation series and the exact equation for the first moment (the mean field), known as the Dyson equation, and for the second moment (the correlation function), the Bethe–Salpeter equations were derived. These equations are exact in the sense that the multiple scattering of all orders, as well as the diffraction and interference effects, are all included in the equations. However, since the operator involved in these equations is in the form of an infinite series, there is no solution available at present. Approximations have to be made to the operator before some practical solutions can be obtained. The most widely used approximation is the first-order smoothing approximation as called by Frisch (1968) (see also Ishimaru 1978a, vol. 2), in

which the local Born approximation of the fluctuating field (or equivalently the bilocal approximation to the mean field) is applied to the Dyson equation and the ladder approximation is applied to the Bethe–Salpeter equation. These approximations can be obtained by either the Feynman diagram method or the Bogoliubov smoothing method in the operator form (Frisch 1968; Tatarskii 1971; Ishimaru 1978a; for the various names of the first-order smoothing approximation, see also Wu 1982b, footnote 2). The justification for the use of this approximation has been clarified by Frisch (1968) by introducing the generalized Reynolds number. The basic physical condition for the valid use of the approximation is the scattered field within a correlation length being weak compared with the incident field. In the case of large-scale inhomogeneities, Fante (1982) has shown that a sufficient condition for applying the ladder approximation is the mean free path for multiple scattering being large in comparison with the correlation length of the medium. This condition is usually satisfied in the context of seismic wave scattering in the lithosphere. (On average the effective mean free path is greater than 100 km, and the correlation length is considered to be less than 10 km for the coda problems, see Aki 1980, Sato 1984 and Wu & Aki 1985b.) The first-order smoothing approximation to the Dyson equation and Bethe–Salpeter equation can be shown (Frisch 1968) to be equivalent to the Foldy–Twersky system of equations, which have been developed independently for discrete random media, i.e. the media with randomly distributed scatterers. There are still no general solutions for these equations and further approximations are needed to put them into practical use. For small size inhomogeneities, there are some general solutions for the mean field, but no useful results for the second moments (Tatarskii 1971, section 61; Ishimaru 1978a, chapter 14). It has been shown that the first-order smoothing approximation of the Dyson and Bethe–Sapeter equations can lead to a radiative transfer equation for the specific intensity which is the 3-D spatial Fourier transform of the spatial correlation function of the wavefield when the correlation function is a slowly varying function in space (Barabanenkov 1969, 1971; Tatarskii 1971, section 63, Ishimaru 1975, 1978a). Similarly, a generalized radiative transfer equation can be derived for the frequency correlation function (Ishimaru 1978a). Thereby the link has been established between the analytic theory and the transport theory.

The second branch of the analytic theory includes all the small angle scattering methods. Because of the small scattering angle approximation or forward-scattering approximation, the basic starting point of the method is the parabolic wave equation. There are two approaches: parabolic equation approach and Feynman path integral approach. Tatarskii applies the Markov approximation to the parabolic wave equation, so the theory of Markov process can be used to study the problem (Tatarskii 1971). Uscinski, on the other hand, uses the plane wave decomposition and phase-screen technique to the parabolic wave equation (Uscinski 1977). At present, the parabolic equation methods can have only approximate solutions for up to the fourth moment equations. The path-integral approach starts with the Feynman path-integral representation of the parabolic wave equation and makes use of the small scattering angle approximation and Markov approximation (Dashen 1977; Flatte *et al.* 1979). It can obtain solutions for any higher-order moments for the Gaussian statistics. Flatte *et al.* have applied this approach to the ocean acoustics and obtained the expressions for phase and intensity fluctuations, various correlations and pulse wandering and spreading etc.

The transport theory (or radiative transfer theory) is a phenomenological approach. It does not start with the wave equation, but deals directly with the energy transport process. Therefore, only energy or intensity arithmetic appears in the theory and no wave interference is considered. This treatment much simplifies the mathematics. Historically it appeared earlier than the analytic theory, and has its root from Boltzmann's equations in the

kinetic theory of gases and in the neutron transport theory. It was introduced into astrophysical optics by Schuster (1905), Chandrasekhar (1950) and others and is now widely used in the multiple scattering treatment in the astrophysical optics, ocean acoustics, neutron transport theory, electromagnetic wave remote sensing, marine biology, etc. (Chandrasekhar 1950; Sobolev 1963; Menzel 1966; Davison 1957; Bell & Glasstone 1970; Flatte *et al.* 1979; Kong, Tsang & Shin 1984; Jerlov 1976). This approach also has its shortcomings. It can only deal with the second moments, it does not account for the diffraction and interference phenomena. Neglecting interference may lead to some problems of energy unbalance in the local region by single scattering, but the overall energy conservation will be taken care of by the multiple scattering treatment. One example for impenetrable reflectors is given in the Appendix. However, there are some new developments, which incorporate some wave interference effects into the radiative transfer equation. For example, in deriving the transfer equations from the Bethe–Salpeter equation, beside the ladder terms (which alone will lead to the regular intensity transfer equation), the cyclical diagrams are also included, resulting in a modified radiative transfer equation, which can account for the backscattering enhancement due to the constructive interference effect caused by the double passage of the backscattered waves (Zuniga, Kong & Tsang 1980). So-called 'wave radiative transfer theory' based on the second-order approximations to the Bethe–Salpeter equation is also under development (Tsang & Ishimaru 1985).

For the coda envelopes or coda energy problems of local earthquakes, it is apparently a wide-angle scattering problem, so that the transport theory is probably the most effective method to treat it at present. In this paper we use the frequency domain formulation mainly from the neutron transport theory and the electromagnetic wave propagation (Davison 1957; Liu & Ishimaru 1974; Fante 1973, Ishimaru 1978b) to the energy density decay with distance of the seismic waves from local earthquakes, and discuss the possibility of using the decay curves to evaluate the relative strengths of the intrinsic absorption and the scattering coefficient of the medium in the region studied. In the second part of the paper (in preparation), we will apply the theory to the Hindu Kush data and discuss the results and their geophysical meaning.

2 Definitions and notations

It is difficult to keep all the notations and terminology in radiative transfer theory without causing ambiguities and contradictions with the traditional notation and terminology in seismology when the theory is introduced into seismology. I will basically follow Ishimaru (1978a) and make some necessary changes to keep the notations self-consistent.

$I(\mathbf{r}, \hat{\Omega})$: *Specific intensity or directional intensity.* It is the most fundamental quantity in transport theory. It gives the power flowing within a unit solid angle in the direction $\hat{\Omega}$, here $\hat{\Omega}$ is the unit vector, emanated from a unit area perpendicular to $\hat{\Omega}$, in a unit frequency band. The specific intensity is defined for a frequency ω, which is omitted in the notation.

In this paper we consider the *S*-wave and its coda for small local earthquakes. Since the *P*-wave energy is much smaller than the *S*-wave energy for a double-couple point source which is the source model for small earthquakes, we consider here $I(\mathbf{r}, \hat{\Omega})$ as only the *S*-wave energy by neglecting the mode converted energy from *P*-waves. We assume here also that the wave energy described by $I(\mathbf{r}, \hat{\Omega})$ is depolarized, i.e. the energy is equally partitioned between the two orthogonal components of *S*-waves. This agrees generally with the observations. Because of the free surface reflection and the scattering by heterogeneities, the *S*-waves from a double-couple source get quickly depolarized. From the results of this paper,

the energy density decay curves for the two orthogonal components are very similar to each other, which further validate the assumptions.

In order to measure the specific intensity (or directional intensity), we need strongly directional sensors, which are not available in the seismological practice. Therefore the specific intensity is not the quantity measured in practice, but is the important concept and quantity for theoretical derivations.

$\bar{I}(\mathbf{r})$: *Average intensity*, defined by

$$\bar{I}(\mathbf{r}) = \frac{1}{4\pi} \int_{4\pi} I(\mathbf{r}, \hat{\Omega})\, d\Omega, \tag{2.1}$$

is the intensity at point $\mathbf{r}$ averaged over all directions.

$E(\mathbf{r})$: *Energy density*, defined by

$$E(\mathbf{r}) = \frac{1}{C} \int_{4\pi} I(\mathbf{r}, \hat{\Omega})\, d\Omega = \frac{4\pi}{C} \bar{I}(\mathbf{r}) \tag{2.2}$$

where C is the wave velocity. This quantity can be measured in practice. In this paper, we will formulate equations for $E(\mathbf{r})$ and obtain solutions for some cases.

$\mathbf{J}(\mathbf{r})$: *Flux density vector*, defined by

$$\mathbf{J}(\mathbf{r}) = \int_{4\pi} I(\mathbf{r}, \hat{\Omega})\, \hat{\Omega}\, d\Omega. \tag{2.3}$$

The net flux density in a particular direction $\hat{\Omega}_0$ is defined as $\hat{\Omega}_0 \cdot \mathbf{J}(\mathbf{r})$. It is the net power transferred along the $\hat{\Omega}_0$ direction across a unit area perpendicular to $\hat{\Omega}_0$. In this paper, we also use the notation for the energy flux density, i.e. the power flux density divided by the wave velocity c.

$S(\hat{\Omega}, \hat{\Omega}_0)$: *Scattering intensity function* of a random medium, which is related to the *single scattering amplitude* $f(\hat{\Omega}, \hat{\Omega}_0)$ of an elementary volume dV of the inhomogeneous medium by

$$S(\Omega, \Omega_0) = \frac{\langle |f(\hat{\Omega}, \hat{\Omega}_0)|^2 \rangle}{dV}, \tag{2.4}$$

where $\langle\ \rangle$ denotes taking ensemble average. $S(\hat{\Omega}, \hat{\Omega}_0)$ gives the scattered power in the $\hat{\Omega}$ direction within a unit solid angle by a unit volume of the random medium for a unit power flux density of incident wave in the $\hat{\Omega}_0$ direction.

In this paper we will give a unified treatment for both the discrete and the continuous random media. For a discrete random medium composed of randomly distributed scatterers, $S(\hat{\Omega}, \hat{\Omega}_0)$ is defined by the scattering characteristics of individual scatterers; while in the case of random continua, we can choose the volume elements small enough so that we can derive the single scattering amplitude $f(\hat{\Omega}, \hat{\Omega}_0)$ by the Born approximation.

$g(\hat{\Omega}, \hat{\Omega}_0)$: *Directional scattering coefficient*, defined by

$$g(\hat{\Omega}, \hat{\Omega}_0) = 4\pi S(\hat{\Omega}, \hat{\Omega}_0). \tag{2.5}$$

for the definition and the derivation for elastic random media, see Wu & Aki (1985b).

$\eta_s \equiv g$: *Scattering coefficient* of the medium defined by

$$\eta_s = \int_{4\pi} S(\hat{\Omega}, \hat{\Omega}_0)\, d\hat{\Omega} = \frac{1}{4\pi} \int_{4\pi} g(\hat{\Omega}, \hat{\Omega}_0)\, d\hat{\Omega}, \tag{2.6}$$

which gives the total power loss due to scattering by a unit volume random medium per unit power flux density of incident wave under the single scattering assumption.

$\eta_a \equiv b$: *Absorption coefficient* of the medium, which gives the power loss due absorption by a unit volume random medium per unit power flux density of incident wave.

η_e: *Extinction coefficient* of the medium, defined by

$$\eta_e = \eta_a + \eta_s. \tag{2.7}$$

$l_0 \equiv a$: *Correlation length* of the random medium.
$L_e = 1/\eta_e$: *Extinction length* of the medium.
$L_a = 1/\eta_a$: *Absorption length* of the medium.
$L_s = 1/\eta_s$: *Scattering length* or *scattering mean free path* of the medium. (2.8)

D_e: *Numerical extinction distance,* which is called 'optical distance' in optics.
D_a: *Numerical absorption distance.*
D_s: *Numerical scattering distance,* defined by

$$D_e = r/L_e,$$

$$D_a = r/L_a,$$

$$D_s = r/L_s, \tag{2.9}$$

where r is the travel distance.

B_0: *Medium seismic albedo,* defined by

$$B_0 = \frac{\eta_s}{\eta_e} = \frac{\eta_s}{\eta_s + \eta_a}. \tag{2.10}$$

$D(\hat{\Omega}, \hat{\Omega}_0)$: *Scattering directivity,* defined by

$$D(\hat{\Omega}, \hat{\Omega}_0) = \frac{g(\Omega, \Omega_0)}{\eta_s} = \frac{4\pi S(\Omega, \Omega_0)}{\eta_s}. \tag{2.11}$$

It is the normalized directional scattering coefficient, and satisfies

$$\frac{1}{4\pi} \int_{4\pi} D(\hat{\Omega}, \hat{\Omega}_0) = 1, \tag{2.12}$$

that means its average over all the directions is equal to unit. In the case of isotropic scattering

$$D(\hat{\Omega}, \hat{\Omega}_0) \equiv 1. \tag{2.13}$$

Its relation with the 'phase function' in the radiative transfer theory (Chandrasekhar 1960; Ishimaru 1978b) is

$$D(\hat{\Omega}, \hat{\Omega}_0) = B_0 p(\hat{\Omega}, \hat{\Omega}_0). \tag{2.14}$$

$p(\hat{\Omega}, \hat{\Omega}_0)$: *Phase function* (see 2.14).

In the case of a discrete random medium having statistically uniformly distributed random scatterers with number density n, we have

$\sigma_d(\hat{\Omega}, \hat{\Omega}_0)$: *Differential (or directional) scattering cross-section* of the scatterers.

$$S(\hat{\Omega}, \hat{\Omega}_0) = n\sigma_d(\hat{\Omega}, \hat{\Omega}_0). \tag{2.15}$$

σ_s: *Scattering cross-section of the scatterers,* defined by

$$\sigma_s = \int_{4\pi} \sigma_d(\Omega, \hat{\Omega}_0)\, d\Omega. \tag{2.16}$$

σ_a: *Absorption cross-section of the scatterers.*

$\sigma_t = \sigma_s + \sigma_a$: *Total cross-section of the scatterers.*

η_h: *Absorption coefficient of the host medium.*

$$\eta_s = n\sigma_s, \tag{2.16}$$

$$\eta_a = n\sigma_a + \eta_h, \tag{2.17}$$

$$D(\hat{\Omega}, \hat{\Omega}_0) = \frac{4\pi\sigma_d(\hat{\Omega}, \hat{\Omega}_0)}{\sigma_s}. \tag{2.18}$$

B_1: *Scatterer albedo,* defined by

$$B_1 = \frac{\sigma_s}{\sigma_s + \sigma_a} = \frac{\sigma_s}{\sigma_t}. \tag{2.19}$$

Therefore,

$$B_0 = \frac{\eta_s}{\eta_s + \eta_a} = \frac{n\sigma_s}{n\sigma_s + n\sigma_a + \eta_h} = \frac{n\sigma_s}{n\sigma_t + \eta_h}. \tag{2.20}$$

When $\eta_h \ll n\sigma_t$, we have

$$B_0 \approx \frac{\sigma_s}{\sigma_t}\left(1 - \frac{\eta_h}{n\sigma_t}\right) = B_1\left(1 - \frac{\eta_h}{n\sigma_t}\right). \tag{2.21}$$

For a perfect scattering medium $B_0 = 1$.

3 Energy density distribution in the case of isotropic scattering

Knowing the extinction coefficient and scattering coefficient of the medium η_e, η_s and the scattering directivity $D(\hat{\Omega}, \hat{\Omega}_0)$ or the scattering intensity function of the medium $S(\hat{\Omega}, \hat{\Omega}_0)$ defined by (2.6), (2.7), (2.11) and (2.4), we can obtain the differential equation for the specific intensity $\mathbf{I}(\mathbf{r}, \hat{\Omega})$, the 'equation of transfer' (Chandrasekhar 1960; Ishimara 1978a, chapter 7):

$$\frac{dI(\mathbf{r}, \hat{\Omega})}{dl} = -\eta_e I(\mathbf{r}, \hat{\Omega}) + \int_{4\pi} S(\hat{\Omega}, \hat{\Omega}_0) I(\mathbf{r}, \hat{\Omega}_0)\, d\Omega_0 + W(\mathbf{r}, \hat{\Omega})$$

$$= -\eta_e I(\mathbf{r}, \hat{\Omega}) + \frac{\eta_s}{4\pi}\int_{4\pi} D(\hat{\Omega}, \hat{\Omega}_0) I(\mathbf{r}, \hat{\Omega}_0)\, d\Omega_0 + W(r, \hat{\Omega}), \tag{3.1}$$

where $W(\mathbf{r}, \hat{\Omega})$ is the source intensity function, which defines the amount of power emitted from the sources into the direction $\hat{\Omega}$ per unit solid angle. In (3.1), dl is the length of a cylindrical elementary volume of unit cross-section in the medium with the axis of the

cylinder in the $\hat{\Omega}$ direction (Fig. 1). Therefore the left side of (3.1) represents the total change of the specific intensity for a unit travel distance. The first term in the right side of (3.1) is the loss of power in the $\hat{\Omega}$ direction due to absorption and scattering, whereas the second term gives the gain of power in that direction from the scattered waves for the incident intensity from all directions, and the third term is the energy supply from the sources. No general analytic solutions are available for (3.1). Some methods such as the

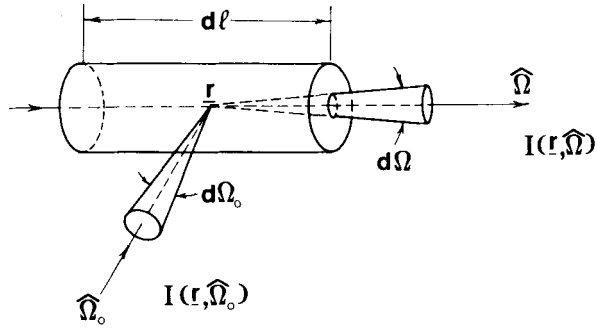

Figure 1. The derivation of the transfer equation for the specific intensity $I(\mathbf{r}, \hat{\Omega})$.

Gauss-quadrature can be used to obtain the numerical solutions for a general scattering function. Let us first consider the simplest case of isotropic scattering. In this case the scattering directivity $D(\hat{\Omega}, \hat{\Omega}_0) \equiv 1$. Integrating (3.1) over all directions $\hat{\Omega}$, we obtain an equation for the average intensity $\bar{I}(\mathbf{r})$ or the energy density $E(\mathbf{r})$ (2.2)

$$\frac{dE(\mathbf{r})}{dl} = -\eta_e E(\mathbf{r}) + \frac{1}{C}\int_{4\pi}\left[\frac{\eta_s}{4\pi}\int_{4\pi} I(\mathbf{r}, \hat{\Omega}_0)\,d\Omega_0 + W(\mathbf{r}, \hat{\Omega})\right] d\Omega$$

$$= -\eta_e E(\mathbf{r}) + Q(l), \tag{3.2}$$

where C is the wave velocity. Equation (3.2) is in a form of first-order differential equation, in which the second term in the right side is the source term

$$Q(l) = \frac{1}{C}\int_{4\pi}\left[\frac{\eta_s}{4\pi}\int_{4\pi} I(\mathbf{r}, \hat{\Omega}_0)\,d\Omega_0 + w(\mathbf{r}, \hat{\Omega})\right] d\Omega. \tag{3.3}$$

The general solution for (3.2) is

$$E(\mathbf{r}) = A\exp(-\eta_e l) + \int_0^l Q(l_1)\exp[-\eta_e(l - l_1)]\,dl_1, \tag{3.4}$$

where A is a constant. Note that (3.4) is in fact an integral equation, since $Q(l)$ has an unknown function $I(\mathbf{r}, \hat{\Omega}_0)$. In the following we will solve the equation.

The energy density (3.4) is composed of two terms. The first term is a simple exponential decay with the extinction coefficient η_e as its attenuation coefficient; this is the coherent energy density E_c or 'reduced energy density' (Ishimaru 1978b). The second term is therefore the diffuse energy density E_d which is produced by scattering. Applying the initial condition

$$E(\mathbf{r}_0) = E_{in}, \tag{3.5}$$

where E_{in} is the incident energy, we get

$$E(\mathbf{r}) = E_c(\mathbf{r}) + E_d(\mathbf{r})$$

$$E_c(\mathbf{r}) = E_{in} \exp(-\eta_e l)$$

$$E_d(\mathbf{r}) = \int_0^l Q(l_1) \exp[-\eta_e(l - l_1)] dl_1$$

$$= \frac{1}{C} \int_0^l \int_{4\pi} \left[\frac{\eta_s}{4\pi} \int_{4\pi} I(\mathbf{r}, \hat{\Omega}_0) d\Omega_0 + W(\mathbf{r}, \hat{\Omega}) \right] \exp[-\eta_e(l - l_1)] d\Omega dl_1. \tag{3.8}$$

In order to calculate the diffuse term (3.8), we need to know the intensity $I(\mathbf{r}, \hat{\Omega}_0)$ which is related to the total energy density. Therefore (3.8) is in the form of an integral equation. To carry out the integration with respect to $\hat{\Omega}$, we note that the intensity gain in the direction $\hat{\Omega}$ within $d\Omega$ is contributed from the intensity of all the volume elements dV_1 at $\mathbf{r}_1$ within the elementary solid angle, and

$$dV_1 = d\Omega |\mathbf{r} - \mathbf{r}_1|^2 dl_1. \tag{3.9}$$

Therefore (3.8) becomes

$$E_d(\mathbf{r}) = \int_V \left[\eta_s E(\mathbf{r}_1) + \frac{4\pi}{C} W(\mathbf{r}_1, \hat{\Omega}) \right] \frac{\exp(-\eta_e |r - r_1|)}{4\pi |\mathbf{r} - \mathbf{r}_1|^2} dV_1. \tag{3.10}$$

The integration is over the volume of the random medium. The integral equation for the total energy density becomes (see also Ishimaru 1978b, chapter 12).

$$E(\mathbf{r}) = E_{in} \exp(-\eta_e l) + \int_V [\eta_s E(\mathbf{r}_1) + \epsilon(\mathbf{r}_1, \Omega)] G_0(\mathbf{r} - \mathbf{r}_1) dV_1, \tag{3.11}$$

where

$$\epsilon(\mathbf{r}, \hat{\Omega}) = \frac{4\pi}{C} W(\mathbf{r}_1, \hat{\Omega}) \tag{3.12}$$

is the source energy density function, and

$$G_0(\mathbf{r} - \mathbf{r}_1) = \frac{\exp(-\eta_e R)}{4\pi R^2} = \frac{\exp(-\eta_e |r - r_1|)}{4\pi |r - r_1|^2}. \tag{3.13}$$

Integral equation (3.11) can also be derived from the first-order smoothing approximation of the Dyson and Bethe–Salpeter equations (Liu & Ishimaru 1974).

From (3.11), the energy density $E(\mathbf{r})$ is totally defined by the incident field, the source function, and the volume of the random medium. For the problems of seismic coda waves of local earthquakes, the distances between the stations and the sources are short compared with the travel times of coda waves. As the first approximation, we consider the problem of a point source located in an infinite randomly inhomogeneous medium. The effect of the free surface is like a mirror reflecting the half random space to a whole random space with the upper half-space being the mirror image of the lower half-space. The limited thickness of the lithosphere, which is supposed to be more heterogeneous than the asthenosphere beneath, will have influence on the later part of the coda. Further discussion about the limitation of the model will be given later in this paper.

In (3.11), suppose the incident field $E_{in} = 0$ and the point source is located at $\mathbf{r} = 0$, radiating the total power P_0. Then

$$\epsilon(\mathbf{r}) = \frac{P_0}{C}\delta(\mathbf{r}) = E_0\delta(\mathbf{r}). \tag{3.14}$$

The equation (3.11) becomes

$$E(\mathbf{r}) = E_0 \frac{\exp(-\eta_e r)}{4\pi r^2} + \int_V \eta_s E(\mathbf{r}_1) \frac{\exp(-\eta_e |\mathbf{r} - \mathbf{r}_1|)}{4\pi |\mathbf{r} - \mathbf{r}_1|^2} dV_1$$

$$= E_0 G_0(\mathbf{r}) + \int_V \eta_s E(\mathbf{r}_1) G_0(\mathbf{r} - \mathbf{r}_1)\, dV_1. \tag{3.15}$$

This is a Faltung type or convolution type integral equation (Tricomi 1957; Carrier, Krook & Pearson 1966) and a Fourier transform method can be used for its solution. Assuming $E_0 = 1$, the solution can be written as (see Davison 1957; Liu & Ishimaru 1974; Ishimaru 1978a, equation 12–21))

$$E(\mathbf{r}) = \frac{\eta_e P_d}{4\pi r}\exp(-\eta_e d_0 r) + \frac{\eta_e}{4\pi r}\int_1^\infty f(s, B_0)\exp(-\eta_e r s)\, ds$$

$$= E_d(r) + E_c(r), \tag{3.16}$$

where

$$P_d = \frac{2d_0^2(1 - d_0^2)}{B_0(d_0^2 + B_0 - 1)}, \tag{3.17}$$

and d_0 is the diffuse multiplier determined by

$$\frac{B_0}{2d_0}\ln\left(\frac{1 + d_0}{1 - d_0}\right) = 1; \tag{3.18}$$

and

$$f(s, B_0) = \left\{\left[1 - \frac{B_0}{s}\tanh^{-1}\left(\frac{1}{s}\right)\right]^2 + \left(\frac{\pi}{2}\frac{B_0}{s}\right)^2\right\}^{-1}. \tag{3.19}$$

The first term in (3.16) is the diffuse term E_d, which is attributed to the pole residue in the complex spatial frequency plane, and the second coherent term E_c, is from the branch cut integration.

Fig. 2 shows the relation between the diffuse multiplier d_0 and the medium albedo B_0. d_0 is always less than 1. When the distance r is large, especially for large B_0, the diffuse term becomes dominant (see also Fig. 9), and $E(r)$ will be approximately an exponential decay with an apparent attenuation coefficient $d_0\eta_e$, which is less than the extinction coefficient η_e. The degree of reduction depends on the albedo B_0. The diffuse term can also be written as

$$E_d(r) = \frac{\eta_e P_d}{4\pi r}\exp[-(\eta_a + d_s\eta_s)r],$$

$$d_s = \frac{d_0 - (1 - B_0)}{B_0}. \tag{3.20}$$

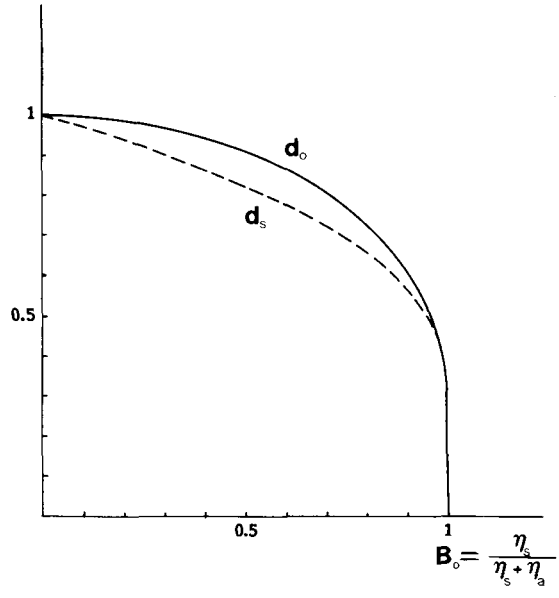

Figure 2. The diffuse multipliers d_0 and d_s as functions of B_0 (the medium seismic albedo).

Table 1. The diffuse multipliers d_0 and d_s.

B_0	0.1	0.2	0.3	0.4	0.5	0.6	0.7	0.8	0.9	0.95	0.99
d_0	0.997	0.987	0.969	0.944	0.910	0.866	0.807	0.728	0.611	0.519	0.374
d_s	0.97	0.94	0.90	0.86	0.82	0.78	0.72	0.66	0.57	0.49	0.37

d_s is a multiplier and $d_s\eta_s$ gives the effective contributions of the scattering coefficient to the apparent attenuations. d_s is also plotted in Fig. 2. Table 1 lists some values of d_0 and d_s versus B_0.

The coherent term can also be written as

$$E_c(r) = \frac{\eta_e}{4\pi r} \int_0^1 f(\xi, B_0) \exp\left(-\frac{\eta_e r}{\xi}\right) \frac{d\xi}{\xi^2}, \tag{3.21}$$

by setting $\xi = 1/s$ for the convenience of computation. Fig. 3 shows the behaviour of the two factors of the integrand for different numerical extinction distances $D_e = \eta_e r$ and different medium albedo B_0. $\exp(-D_e/\xi)/\xi^2$ has a sharp peak for small D_e when ξ is small; whereas $f(\xi, B_0)$ is nearly singular for small B_0 when ξ is close to 1. Therefore, in doing numerical integration, we used Romberger's integration method for three separate segments to take care of the abrupt changes of the integrand at both ends of the interval. The Gauss–Legendre quadrature is also used to check the results. It turned out that the Gauss–Legendre quadrature of order 10 gives fairly good results.

In the following we will show some numerical results of the energy density distribution along the travel path from the source point. In the case of homogeneous media, the decay of energy density with distance is only due to geometric spreading. For a isotropic point source, the decay is $1/4\pi r^2$. Therefore, we normalize the distribution for inhomogeneous

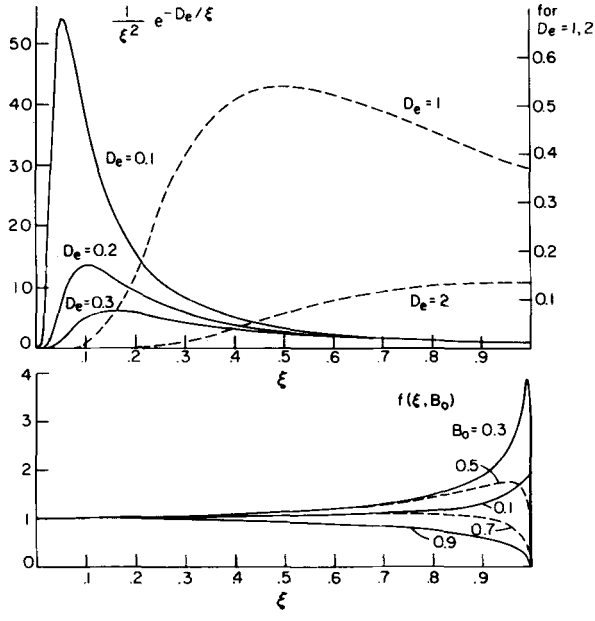

Figure 3. The behaviour of the integrand of the integral for the coherent term.

media (3.16) by the homogeneous distribution, i.e. multiply both sides of (3.16) with $4\pi r^2$,

$$E_n(r) = 4\pi r^2 E(r) = \eta_e P_d r \exp(-\eta_e d_0 r) + \eta_e r \int_0^1 f(\xi, B_0) \exp\left(-\frac{\eta_e r}{\xi}\right)\frac{d\xi}{\xi^2}$$

$$= D_e P_d \exp(-d_0 D_e) + D_e \int_0^1 f(\xi, B_0) \exp(-D_e/\xi)\frac{d\xi}{\xi^2}, \tag{3.22}$$

where $E_n(r)$ stands for the normalized energy density distribution. Fig. 4 gives the results for different medium albedo B_0. The diffuse term and the coherent term are also plotted in the figure for comparison. The coherent term has little changes for different B_0, whereas the diffuse term varies dramatically with B_0, especially when $B_0 > 0.5$, i.e. when scattering is dominant. This gives the possibility of using the energy density decay curves to calculate the extinction coefficient η_e and the medium albedo B_0, hence to separate the absorption coefficient η_a and the scattering coefficient η_s. In the case of $B_0 > 0.5$, the diffuse term is dominant. There will be a peak on the $E(r)$ curve, the position of the peak will depend on η_e and B_0 of the medium. When $B_0 < 0.5$, the coherent term is dominant for $D_e < 2$. Therefore the shape of the curve is not very sensitive to the change of B_0, so that the separation of scattering from absorption becomes difficult.

By assuming a point source with $E_0 = 1$, we get $E(r)$ around the peak with values greater than 1, that need some explanation. As shown in Fig. 5, the normalized energy density $E_n(r) = 4\pi r^2 E(r)$ represents the energy received by the ring shell (hatched). In a homogeneous medium, if there is no absorption, the energy received will be equal to the source energy. In a scattering medium, the wave energy can go outward and inward across the shell. We denote the outward energy flux by F_r^+ and the inward energy flux by F_r^-. In the figure we sketched one possible path of multiple scattering. No matter how complicated the path is and how long the time delay is compared to the direct path, the closed ring shell will eventually receive all the energy emitted by the source. There is no escape! Therefore, in this

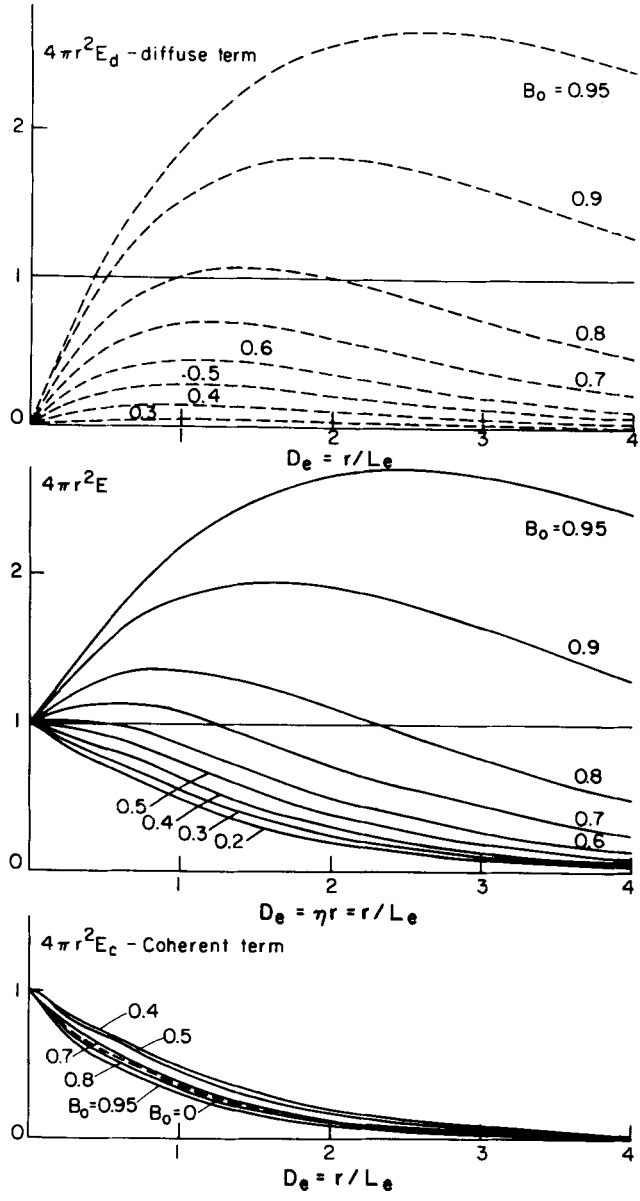

Figure 4. The normalized energy density distribution curves $4\pi r^2 E(r)$, where r is the propagation distance from the point source. At the top are the curves of the diffuse term, at the bottom are those of the coherent term; in the middle are the curves of the sum of the two terms. Here D_e is the numerical extinction distance, $L_e = 1/\eta_e$ is the extinction length of the medium, $\eta_e = \eta_s + \eta_a$ is the extinction coefficient, where η_s and η_a are the scattering coefficient and the absorption coefficient respectively. $B_0 = \eta_s/(\eta_s + \eta_a)$ is the medium seismic albedo.

case the F_r^+ is equal to the total energy. However, the shell will also receive the inward scattered energy, so the total received energy $F_r^+ + F_r^-$ is greater than E_0. Of course the net energy flux $F_r^+ - F_r^-$ is always less than E_0. If there exists absorption, the amount of received energy will depend on the energy balance between the absorption loss and the inward-scattering gain. Near the source, r is small, the ring shell has a small surface area for receiving

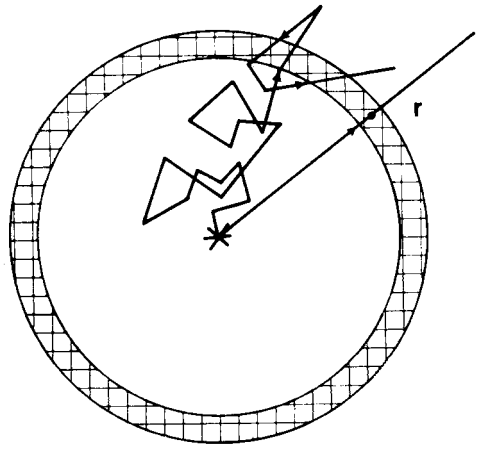

Figure 5. The schematic diagram of a possible multiple scattering path compared with the direct path. The hatched shell of unit thickness will receive the energy $4\pi r^2 E(r)$.

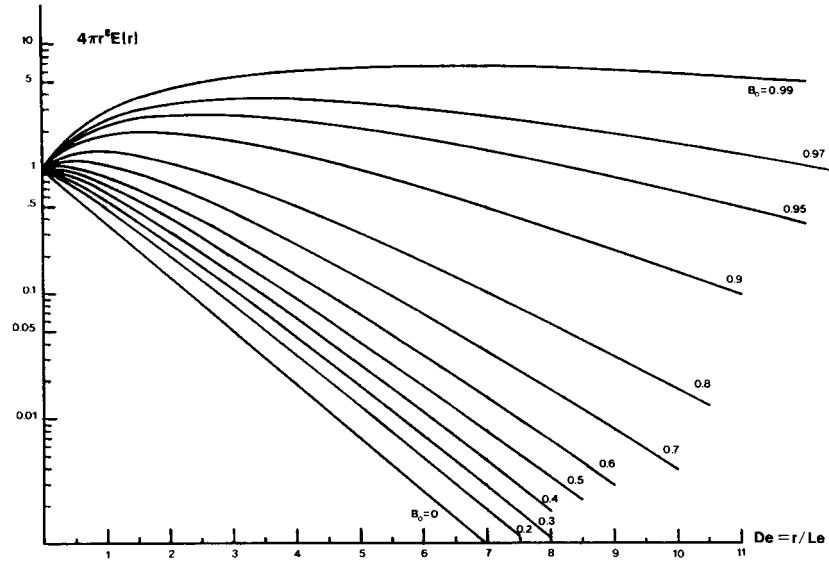

Figure 6. The normalized energy distribution curves $4\pi r^2 E(r)$ in the semi-logarithmic scale.

the inward-scattered energy, so $E_n(r) \approx E_0$. When r increases, the surface area of the shell also increases, so that more inward-scattered energy can be received, resulting in the growth of $E_n(r)$. However, the absorption loss also grows with r due to the increase of the path length. Up to some distance r, the growth rate of gain is equal to the growth rate of loss and the curve reaches its maximum. Beyond this distance, the absorption loss prevails.

Fig. 6 replots the curves of Fig. 4 in a semi-logarithm coordinate system. Figs 7 and 8 plot some $E_n(r)$ curves for cases of constant absorption and constant scattering respectively. In this paper $b \equiv \eta_a$, $g \equiv \eta_s$. Fig. 7 shows the influence of different scattering coefficients on the energy density distribution curve of a constant absorption medium. The distance is normalized by the absorption length of the medium $L_a = 1/\eta_a$. It is seen from the figure that, for large distances compared with the absorption length of the medium, the decay of the

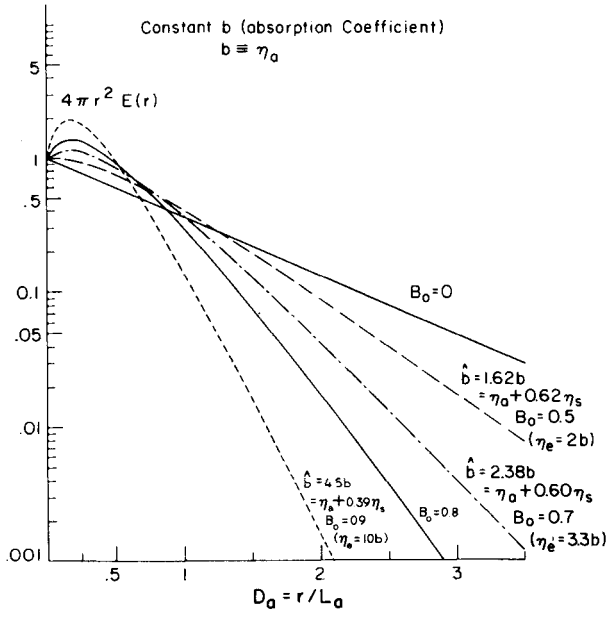

Figure 7. The energy distribution curves with the numerical absorption distance $D_a = r/L_a$, where $L_a = 1/\eta_a$ is the absorption length of the medium. $\hat{b}$ is the apparent attenuation coefficient obtained from the slope of the curve. B_0 is the medium albedo.

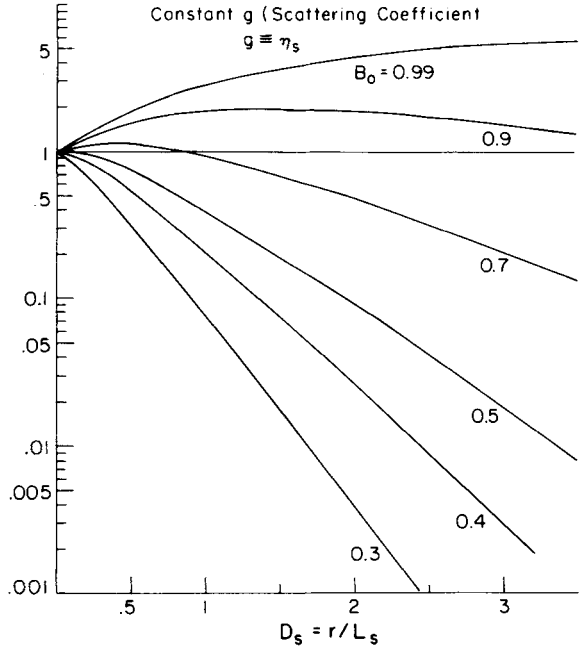

Figure 8. The energy distribution curves with the numerical scattering distance $D_s = r/L_s$, where $L_s = 1/\eta_s$ is the scattering length of the medium. B_0 is the medium albedo.

energy density is nearly exponential with an apparent attenuation coefficient different from both the extinctions coefficient and the absorption coefficient. In the figure, b is the true absorption coefficient and $\hat{b}$ is the apparent attenuation coefficient measured from the slope of the curve. It can be seen that, for strong scattering ($B_0 > 0.5$), the apparent attenuation is much bigger than the absorption coefficient but much smaller than the extinction coefficient (for $B_0 = 0.9$, $\hat{b} = 4.5b = 0.45\,\eta_e$). For weak scattering ($B_0 < 0.5$), the influence of scattering to the apparent attenuation is less appreciable. When $B_0 = 0.5$, $\hat{b} = 1.62b$. On the other hand, for small absorption distance ($D_a \leqslant 1$), the shape of the $E(r)$ curve varies drastically depending on the values of B_0, which provides the basis for the separation of the scattering and absorption effects. Fig. 8 in a similar way shows the influence of absorption on the $E(r)$ curve of a constant scattering medium.

In order to compare the relative contributions of the diffuse term and the coherent term, we plot them on Figs 9 and 10 with the distance normalized by the extinction length L_e and scattering length L_s respectively.

Now, we will derive the radial energy flux density $J_r(r)$. We know the energy conservation relation (see Ishimaru 1978a, equation 7.28)

$$\operatorname{div} \mathbf{J}(\mathbf{r}) = -\frac{\eta_a}{C}\int_{4\pi} I(\mathbf{r}, \hat{\Omega})\, d\Omega + \frac{1}{C}\int_{4\pi} W(\mathbf{r}, \hat{\Omega})\, d\Omega, \tag{3.23}$$

where $J(\mathbf{r})$ is the energy flux density vector, C is the wave velocity and $W(\mathbf{r}, \hat{\Omega})$ is the source intensity. For isotropic scattering in the source-free region

$$\operatorname{div} \mathbf{J}(\mathbf{r}) = \eta_a E(r). \tag{3.24}$$

In view of the spherical symmetry, there is no transverse component of $\mathbf{J}(\mathbf{r})$, therefore (3.24) becomes

$$\operatorname{div} \mathbf{J}(\mathbf{r}) = \frac{1}{r^2}\frac{\partial}{\partial r}(r^2 J_r) = -\eta_a E(r). \tag{3.25}$$

Then

$$J_r = -\frac{\eta_a}{r^2}\int_0^r E(r) r^2\, dr = \frac{\eta_a}{r^2}\int_r^\infty E(r) r^2\, dr. \tag{3.26}$$

Normalizing J_r by the homogeneous case, we get

$$J_{nr}(r) = 4\pi r^2 J_r(r) = \eta_a \int_r^\infty 4\pi r^2 E(r)\, dr = \eta_a \int_r^\infty E_n(r)\, dr. \tag{3.27}$$

Substituting (3.22) into (3.27) yields

$$J_{nr}(r) = 4\pi r^2 J_r(r)$$

$$= (1 - B_0)\left\{\frac{P_d}{d_0}\left(D_e + \frac{1}{d_0}\right)\exp(d_0 D_e) + \int_0^1 f(\xi, B_0)\left(1 - \frac{D_e}{\xi}\right)\exp(-D_e/\xi)\, d\xi. \tag{3.28}$$

Figs 11 and 12 give some numerical results with the distance normalized by the extinction length and the absorption length respectively, together with the results for the forward scattering approximation (see next section). It can be seen that the radial net flux is always smaller than the source energy E_0. However, the radial energy flux is difficult to measure in the practice of seismology. This is because of the difficulty of separating the inward and

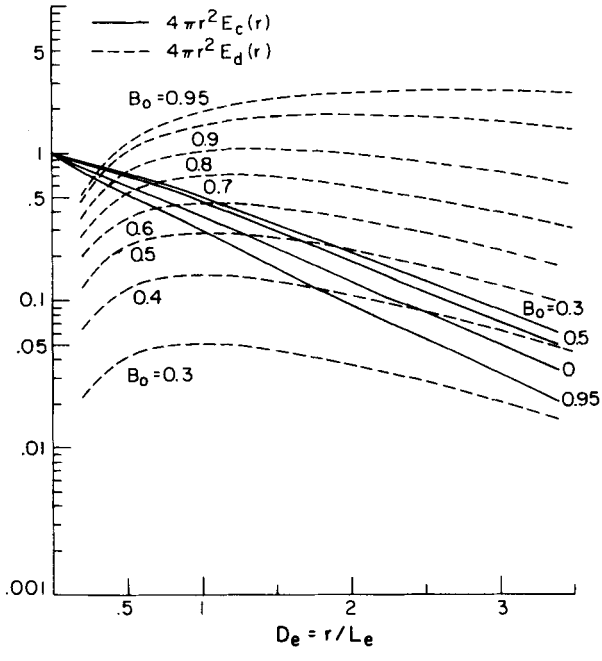

Figure 9. The relative strengths of the diffuse term E_d and the coherent term E_c at different extinction distances $D_e = r/L_e$ for different medium albedo B_0, where $L_e = 1/\eta_e$ is the extinction length of the medium.

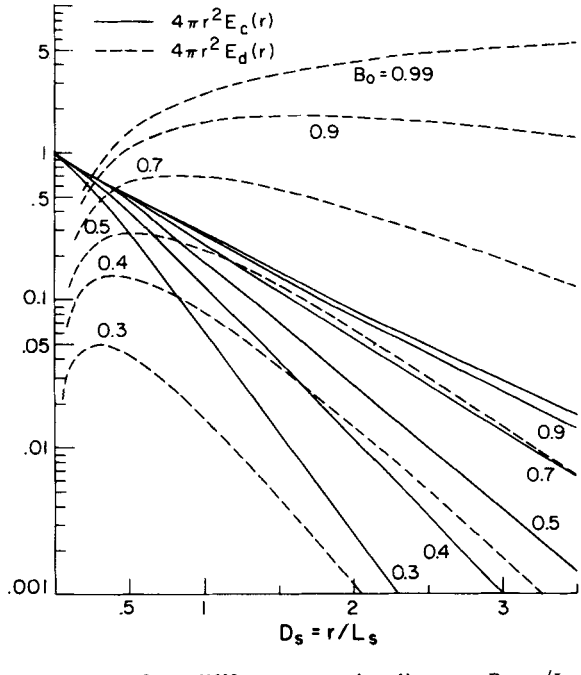

Figure 10. This is the same as Fig. 9, at diffferent scattering distances $D_s = r/L_s$, where $L_s = 1/\eta_s$ is the medium scattering length.

outward energy flows. Nevertheless, the comparison between $E(r)$ and $J_r(r)$ helps us to understand the multiple scattering process.

4 Strong forward scattering: the case of large-scale inhomogeneities

From the analysis of coda generations for local earthquakes, it seems that the lithosphere in tectonically active regions may be rich in small-scale heterogeneities (less than 1 km) (Aki 1981; Wu & Aki 1985b). On the other hand, by measuring the phase and amplitude fluctua-

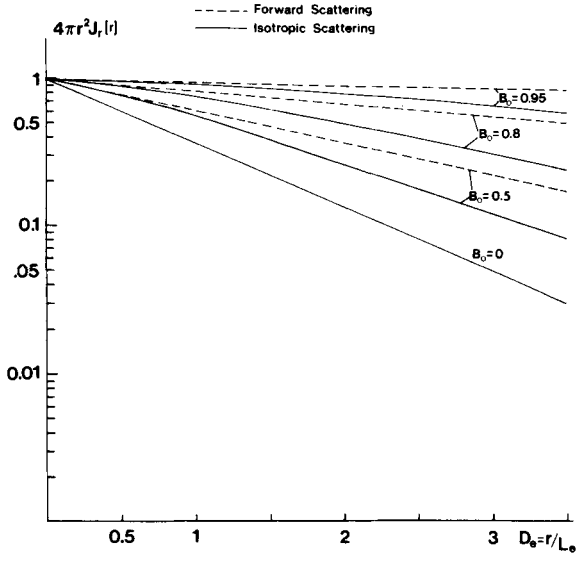

Figure 11. The normalized radial energy flux density $4\pi r^2 J_r(r)$ for the isotropic scattering case and the strong forward scattering case.

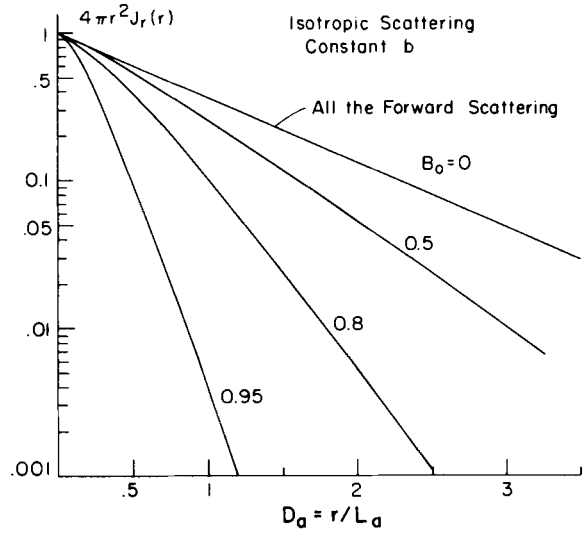

Figure 12. This is the same as Fig. 11. The distance is the numerical absorption distance $D_a = r/L_a$, where $L_a = 1/\eta_a$ is the absorption length of the medium.

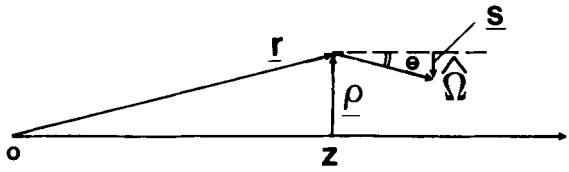

Figure 13. The derivation for the case of the strong forward scattering approximation. z is along the forward direction. $\mathbf{r}$ is the position vector, ρ is the position vector in the transverse plan; $\hat{\Omega}$ is the unit vector in the scattering direction, and $\mathbf{s}$ is the projection of $\hat{\Omega}$ in the transverse plane.

tions in large seismic arrays as LASA and NORSAR, large-scale velocity inhomogeneities (10–20 km) underneath the arrays were revealed (Aki 1973; Capon 1974; Berteusson *et al.* 1975). Therefore, the lithosphere may have multi-scale inhomogeneities. For short-period seismic waves (around 1 Hz), the scattering by the small-scale heterogeneities may be in the Rayleigh and Mie scattering region. From the elastic scattering pattern (Wu & Aki 1985a, b), we may approximately use the isotropic scattering approximation. However, for the large-scale velocity inhomogeneities, the forward scattering is dominant. The energy density distribution with distance will be quite different from the case of isotropic scattering. Since most of the scattered energy is concentrated in the forward direction within a small cone, the focusing and defocusing, diffraction and interference phenomena become important. Most of the scattered energy arrives at the receiver point with much shorter travel paths, so that the energy delay due to scattering is much less severe than in the case of isotropic scattering. From a reasoning similar to that in Fig. 5, we can see that the normalized energy density decay curve will not have a peak value greater than 1. Because the inward scattered energy is much less than the outward scattered energy, the energy density, which is $J_{\mathbf{r}}^{+} + J_{\mathbf{r}}^{-}$, where $J_{\mathbf{r}}^{+}$ and $J_{\mathbf{r}}^{-}$ are the outward and inward radial energy fluxes respectively, will not be too different from the net energy flux $J_{\mathbf{r}} = J_{\mathbf{r}}^{+} - J_{\mathbf{r}}^{-}$. In the following, let us examine what can be obtained from the theory available in transport theory.

Fante (1973) has solved the transport equation under the forward scattering approximation, and Ishimaru (1978a, chapter 13) has a lucid derivation and discussion on it. Here we only draw some main threads for understanding it. Since

$$\frac{dI(\mathbf{r}, \hat{\Omega})}{dl} = \hat{\Omega} \cdot \operatorname{grad} I(\mathbf{r}, \hat{\Omega}), \tag{4.1}$$

where dl is the length of an elementary segment in the $\hat{\Omega}$ direction (Fig. 1), the transport equation (3.1) can be written as

$$\hat{\Omega} \cdot \operatorname{grad} I(\mathbf{r}, \hat{\Omega}) = -\eta_e I(\mathbf{r}, \hat{\Omega}) + \frac{\eta_s}{4\pi} \int_{4\pi} D(\hat{\Omega}, \hat{\Omega}_0) I(\mathbf{r}, \Omega_0)\, d\Omega_0 + W(\mathbf{r}, \hat{\Omega}). \tag{4.2}$$

Because the scattered energy is mostly confined within a small cone in the forward direction, we choose the z-axis of the Cartesian coordinates as this direction, and approximate (4.2) through the following steps.

$$\hat{\Omega} = l\hat{x} + m\hat{y} + n\hat{z}, \tag{4.3}$$

where $\hat{x}$, $\hat{y}$ and $\hat{z}$ are the unit vectors in the x, y and z-axes respectively, and l, m, n, the corresponding direction cosines. In the spherical coordinate system with the z-axis as its polar axis (Fig. 13)

$$l = \sin\theta \cos\phi, \qquad m = \sin\theta \sin\phi \qquad n = \cos\theta.$$

Because the angle with the z-axis θ is always small, we have approximations

$$n = \cos\theta \approx 1$$

$$d\Omega \approx n\,d\Omega = dl\,dm = d\mathbf{s},$$

$$\int_{4\pi} d\Omega \approx \int_{-\infty}^{\infty} dl \int_{-\infty}^{\infty} dm = \int d\mathbf{s},$$

$$\hat{\Omega} \cdot \operatorname{grad} I(\mathbf{r}, \hat{\Omega}) \approx \frac{\partial}{\partial z} I(z, \rho, \mathbf{s}) + \mathbf{s} \cdot \nabla_t I(z, \rho, \mathbf{s}), \tag{4.5}$$

where

$$\mathbf{r} = x\hat{x} + y\hat{y} + z\hat{z} = \rho + z\hat{z},$$

$$\mathbf{s} = l\hat{x} + m\hat{y}, \qquad \nabla_t = \frac{\partial}{\partial x}\hat{x} + \frac{\partial}{\partial y}\hat{y}. \tag{4.6}$$

Note that $\mathbf{s}$ is not a unit vector. Because θ is a small angle, the magnitude of $\mathbf{s}$ is much smaller than 1.

By these approximations (4.2) becomes

$$\frac{\partial}{\partial z} I(z, \rho, \mathbf{s}) + s \cdot \nabla_t I(z, \rho, \mathbf{s})$$

$$= -\eta_e I(z, \rho, \mathbf{s}) + \frac{\eta_s}{4\pi} \int\int_{-\infty}^{\infty} D(\mathbf{s} - \mathbf{s}') I(z, \rho, \mathbf{s}')\, d\mathbf{s}' + W(z, \rho, \mathbf{s}). \tag{4.7}$$

here $D(\hat{\Omega}, \hat{\Omega}_0)$ is assumed only as a function of $\hat{\Omega} - \hat{\Omega}_0$. Since most of the energy is confined within a small angle with the z-axis, the integration limits for l and m are extended to $\pm\infty$ without introducing any significant change.

Again (4.7) can be solved by the Fourier transform method (Fante 1973; Ishimaru 1978a, chapter 13), the general solution for $W(z, \rho, \mathbf{s}) = 0$ is

$$I(z, \rho, \mathbf{s}) = \frac{1}{(2\pi)^4} \int d\mathbf{k} \int d\mathbf{q} \exp(-i\mathbf{k} \cdot \rho - i\mathbf{s} \cdot \mathbf{q})\, I_0(\mathbf{k}, \mathbf{q} + \mathbf{k}z)\, K(z, \mathbf{k}, \mathbf{q}), \tag{4.8}$$

where

$$I_0(\mathbf{k}, \mathbf{q}) = \iint I_0(\rho, \mathbf{s}) \exp(i\mathbf{k} \cdot \rho + i\mathbf{s} \cdot \mathbf{q})\, d\rho\, d\mathbf{s} \tag{4.9}$$

is the double Fourier transform of the incident intensity $I_0(\rho, \mathbf{s})$ at $z = 0$, and

$$K(z, \mathbf{k}, \mathbf{q}) = \exp\left\{\int_0^z \eta_e \left[1 - \frac{B_0}{4\pi} D[\mathbf{q} + \mathbf{k}(z - z')]\right] dz'\right\} \tag{4.10}$$

where

$$D(\mathbf{q}) = \iint_{-\infty}^{\infty} D(\mathbf{s}) \exp(i\mathbf{s} \cdot \mathbf{q})\, d\mathbf{s}. \tag{4.11}$$

There is no general explicit expression for (4.8) for a general scattering directivity $D(s)$. If we approximate the strong forward scattering pattern by a Gaussian function,

$$D(\mathbf{s}) \approx 4\xi \exp(-\xi s^2) \tag{4.12}$$

where ξ is a parameter proportional to $(l_0/\lambda)^2$, and l_0 is correlation length of the random medium, λ is the wavelength, substituting into (4.11) and (4.10) yields

$$D(\mathbf{q}) = 4\pi \exp\left(-\frac{q^2}{4\xi}\right), \tag{4.13}$$

$$K(z, \mathbf{k}, \mathbf{q}) = \exp\left\{ \int_0^z \eta_e \left[1 - B_0 \exp\left(\frac{-q^2}{4\xi}\right)\right] dz' \right\}. \tag{4.14}$$

Since most of the energy is confined within a small cone along the z-axis, we consider the case of a plane incident wave

$$I_0(\rho, \mathbf{s}) = I_0 \delta(\mathbf{s}), \tag{4.15}$$

$$I_0(\mathbf{k}, \mathbf{q}) = (2\pi)^2 I_0 \delta(\mathbf{k}). \tag{4.16}$$

From (4.8) we have

$$I(z, \rho, \mathbf{s}) = \frac{I_0}{(2\pi)^2} \int d\mathbf{k} \int d\mathbf{q} \exp(-i\mathbf{k} \cdot \rho - i\mathbf{s} \cdot \mathbf{q}) \delta(\mathbf{k}) \exp\left[-\eta_e z + \eta_s z \exp\left(\frac{-q^2}{4\xi}\right)\right]. \tag{4.17}$$

When the scattering distance is large, i.e. $\eta_s z \gg 1$, the main contributions to the integral in (4.17) come from the integrands with small qs. We can set

$$\exp\left(\frac{-q^2}{4\xi}\right) \approx 1 - \frac{q^2}{4\xi}. \tag{4.18}$$

Therefore

$$I(z, \rho, \mathbf{s}) \approx \frac{I_0 \xi}{\pi \eta_s z} \exp\left[-\eta_a z - \frac{\xi s^2}{\eta_s z}\right]. \tag{4.19}$$

$$E(z, \mathbf{p}) = J(z, \rho) = \int I(z, \rho, \mathbf{s})\, d\mathbf{s} = I_0 \exp(-\eta_a z). \tag{4.20}$$

We see that, under forward scattering approximation, the energy density decay with distance is only due to the absorption. That is because, in the approximation, we neglect the back-scattering and the path length differences between the direct path and the multiple scattering paths by letting $\cos\theta \approx 1$. In Figs 11 and 12 we plot the energy flux $J(r)$ of strong forward scattering versus that of the isotropic scattering. If we consider the lengthening of travel paths by multiple forward scattering, the decay curve could be somewhere between these two extremes.

Equation (4.19) gives the angle distribution of intensities. The incident wave only has intensity in the z-direction and, after scattering by the medium, the intensities with different directions have a Gaussian distribution and the width of the angle distribution broadens with distance. The loss due to the scattering of energy to other directions is compensated by the gain of scattered energy from other directions. Therefore there is no energy loss except absorption. However, in order to calculate the real energy attenuation, we have to take the backscattered energy into account. Wu (1982a) uses a simple renormalization procedure and sums up all the energy scattered into the back half-space as the energy loss. This procedure is similar to DeWolf's 'cumulative forward-scatter single-backscatter approximation' in calculating the backscattering strength (DeWolf 1971). Since the backscattered energy is much smaller than the forward scattered energy, the second backscattered energy (from the

backward direction into the forward direction) is one order smaller than the single backscattered energy. Therefore the single backscattering loss with the renormalization of the total forward energy could be a reasonable approximation of the scattering attenuation for the harmonic wavefield.

From the above analysis, in the case of strong forward scattering due to large-scale inhomogeneities, the shape of the energy density decay curve is insensitive to the medium albedo B_0 and the separation of scattering attenuation from absorption becomes more difficult. However, because the scattering loss is much smaller than the isotropic case, we can have some constraint on the possible scattering attenuation from the strength of inhomogeneities. The shape of the seismogram envelope in the time domain can also give constraints on the possible values of the albedo B_0. We will discuss this in part II of this paper (in preparation, see also Wu 1984).

5 Conclusion

From the solutions of energy transfer equation for seismic waves we can see that the shape of the spatial distribution curve of seismic energy density depends strongly on the seismic albedo $B_0 = \eta_s/(\eta_s + \eta_a)$, where η_s is the scattering coefficient and η_a is the absorption coefficient of the medium. For isotropic or nearly isotropic scattering, such as in the case of Rayleigh scattering, the energy–distance curve is of arch shape and the position of the peak is a function of the extinction coefficient of the medium $\eta_e = \eta_s + \eta_a$ for the case of $B_0 > 0.5$. Therefore it is possible to calculate η_a and η_s from the value of B_0 and η_e, which can be determined from the measured energy–distance curve for a region using local earthquake data.

For strong forward scattering, such as in the case of large-scale inhomogeneities for short-period seismic waves, the shape of the energy–distance curve is insensitive to the seismic albedo B_0. In this case the separation of the scattering effect and the absorption becomes more difficult. However, since the scattering loss is much smaller than the case of isotropic scattering, we can have some constraint on the value of scattering attenuation. Also the time domain solution for the energy transfer equation can supply further information on the relative strength of scattering attenuation. This will be discussed in part II of the paper (see also Wu 1984).

Acknowledgments

I am grateful to Professor K. Aki for his suggestions, discussions and careful reading of the manuscript. I also thank Professor N. Toksoz for helpful discussions. This research was supported by the Advanced Research Projects Agency of the Department of Defense and was monitored by the Air Force Office of Scientific Research under Contract F49620-83-C-0038.

References

Aki, K., 1973. Scattering of *P* waves under the Montana Lasa, *J. geophys. Res.*, **78**, 1334–1346.

Aki, K., 1980. Scattering and attenuation of shear waves in the lithosphere, *J. geophys. Res.*, **85**, 6496–6504.

Aki, K., 1981. Source and scattering effects on the spectra of small local earthquakes, *Bull. seism. Soc. Am.*, **71**, 1687–1700.

Barabanenkov, Y. N., 1969. On the spectral theory of radiation transport equations, *Soviet Phys. JETP*, **29**, 679–684.

Bell, G. I. & Glasstone, S., 1970. *Nuclear Reactor Theory*, Van Nostrand Reinhold, New York.

Berteussen, K. A., Christoffersson, A., Husebye, E. S. & Dahle, A., 1975. Wave scattering theory in analysis of *P* wave anomalies at NORSAR and LASA, *Geophys. J. R. astr. Soc.*, **42**, 403–417.

Capon, J., 1974. Characterization of crust and upper mantle structure under Lasa as a random medium, *Bull. seism. Soc. Am.*, **64**, 235–266.

Carrier, G. F., Krook, M. & Pearson, C. E., 1966. *Functions of a Complex Variable*, chapter 7, McGraw-Hill, New York.

Chandrasekhar, S., 1960. *Radiative Transfer*, Dover, New York (revised version of 1950).

Dashen, R., 1977. Path integrals for waves in random media *Stanford Res. Inst. Tech. Rep. JSR 76-1*, also *J. Math. Phys.*, **20**, 894–920 (1979).

Davison, B., 1957. *Neutron Transport Theory*, Oxford University Press, London.

DeWolf, D. A., 1971. Electromagnetic reflection from an extended turbulent medium: cumulative forward-scatter single-backscatter approximation, *IEEE Trans. Ant. Prop.*, **AP-19**, 254–282.

Fante, R. L., 1973. Propagation of electromagnetic waves through turbulent plasma using transport theory, *IEEE Trans. Ant. Prop.*, **AP-21**, 750–755.

Fante, R. L., 1982. Sufficient condition for applying the ladder approximation to the multiple scattering of light in random media, *J. opt. Soc. Am.*, **72**, 815–818.

Flatte, S. M., Dashen, R., Munk, W. H., Watson, K. M. & Zachariasen, F., 1979. *Sound Transmission Through a Fluctuating Ocean*, Cambridge University Press.

Frisch, V., 1968. *Wave Propagation in Random Media, Probabilistic Methods in Applied Mathematics*, Vol. 1, pp. 76–198, Academic Press, New York.

Gao, L. S., Lee, L. C., Biswas, N. N. & Aki, K., 1983a. Comparison of the effects between single and multiple-scattering on coda waves for local earthquakes, *Bull. seism. Soc. Am.*, **73**, 377–389.

Gao, L. S., Biswas, N. N., Lee, L. C. & Aki, K., 1983b. Effects of multiple scattering on coda waves in a three-dimensional medium, *Pure appl. Geophys.*, **121**, 3–15.

Hoffman, W. C., 1964. Wave propagation in a general random continuous medium, *Proc. Symp. appl. Math.*, **16**, 117–144.

Ishimaru, A., 1975. Correlation functions of a wave in a random distribution of stationary and moving scatterers, *Radio Sci.*, **10**, 45–52.

Ishimaru, A., 1977. Theory and application of wave propagation and scattering in random media, *Proc. IEEE*, **65**, 1030–1061.

Ishimaru, A., 1978a. *Wave Propagation and Scattering in Random Media*, Vols 1 and 2, Academic Press, New York.

Ishimaru, A., 1978b. Diffusion of a pulse in densely distributed scatterers, *J. opt. Soc. Am.*, **68**, 1045–1050.

Jerlov, M. G., 1976. *Marine Optics*, Elsevier, New York.

Kay, I. & Silverman, R. A., 1958. Multiple scattering by a random stack of dielectric slabs, *Nuovo Cim.*, 9 (10), suppl., 625–645.

Kong, J. A., Tsang, L. & Shin, R., 1984. *Theory of Microwave Remote Sensing*, Wiley, New York.

Kopnichev, Y. F., 1977. The role of multiple scattering in the formation of a seismogram's tail, *Izv. Acad. Sci., USSR, Phys. Solid Earth*, **13**, 394–398.

Liu, J. C. & Ishimaru, A., 1974. Multiple scattering of waves by a uniform random distribution of discrete iotropic scatterers, *J. acoust. Soc. Am.*, **56**, 1995–1700.

Menzel, D. H. (ed.), 1966. *Selected Papers on the Transfer of Radiations*, New York, Dover.

O'Doherty, R. F. & Anstey, N. A., 1971. Reflections on amplitudes, *Geophys. Prospect.*, **19**, 430–458.

Richards, P. G. & Menke, W., 1983. The apparent attenuation of a scattering medium, *Bull. seism. Soc. Am.*, **73**, 1005–1021.

Sato, H., 1984. Attenuation and envelope formation of three-component seismograms of small local earthquakes in randomly inhomogeneous lithosphere, *J. geophys. Res.*, **89**, 1221–1241.

Schuster, A., 1905. Radiation through a foggy atmosphere, *Astrophys. J.*, **2**, 1–22.

Sobolev, V. V., 1963. *A Treatise on Radiative Transfer*, Van Nostrand, Princeton, New Jersey.

Tatarskii, V. I., 1971. The effects of the turbulent atmosphere on wave propagation.

Tricomi, F. G., 1957. *Integral Equations*, pp. 22–26, New York.

Tsang, L. & Ishimaru, A., 1985. *Backscattering enhancement for random discrete scatters*. Preprint.

Uscinski, B. J., 1977. *The Elements of Wave Propagation in Random Media*, McGraw-Hill, New York.

Wu, R. S., 1982a. Attenuation of short period seismic waves due to scattering, *Geophys. Res. Lett.*, **9**, 9–12.

Wu, R. S., 1982b. Mean field attenuation and amplitude attenuation due to wave scattering, *Wave Motion*, **4**, 305–316.

Wu, R. S., 1984. Multiple scattering and energy transfer of seismic waves and the applications of the theory to Hindu Kush region, in Seismic wave scattering and the small scale inhomogeneities in the lithosphere, chapter 4, *PhD thesis*, Massachusetts Institute of Technology, Cambridge.

Wu, R. S. & Aki, K., 1985a. Scattering characteristics of elastic waves by an elastic heterogeneity, *Geophysics*, **50** (4).

Wu, R. S. & Aki, K., 1985b. Elastic wave scattering by a random medium and the small scale inhomogeneities in the lithosphere, *J. geophys. Res.*, to appear.

Zuniga, M., Kong, J. A. & Tsang, L., 1980. Depolarization effects in the active remote sensing of random media, *J. appl. Phys.*, **51**, 2315–2325.

Appendix: the problem of energy conservation for the scattering of impenetrable bodies

The radiative transfer equations deal with the scattered energy and neglect the wave interference effect. This can cause some local inbalance of energy due to single scattering. However, one of the salient features of the energy transfer approach is its conformity with the energy conservation law. The overall energy conservation will be taken care of by the multiple scattering process.

For an impenetrable body, the total field can be written as

$$U = U_0 + U_s, \tag{A1}$$

where U_0 is the incident field and U_s the scattered field. The energy of the total field is proportional to

$$|U|^2 = |U_0 + U_s|^2 = |U_0|^2 + |U_s|^2 + U_0^* U_s + U_0 U_s^*, \tag{A2}$$

where '*' stands for the complex conjugate. In the high-frequency limit there is a shadow in the forward direction due to the impenetrability of the target. Therefore the total field vanishes in the forward direction, which implies

$$U_s = -U_0 \tag{A3}$$

in the forward direction. Substituting (A3) into (A2), we reach the expected result that there is no wave energy in the forward direction since all the incident energy was reflected back. However, if we consider only the scattered energy without taking into account the interference, the forward scattered energy will be the same amount as the incident energy. The total backscattered energy is obviously equal to the incident energy. Therefore the total scattered energy is twice the incident energy, that is why the high-frequency limit of the scattering cross-section of an impenetrable target is twice the geometric cross-section. The energy conservation law is violated here. However, it is a problem for the single scattering treatment. The radiative transfer equations, which deal with the multiple scattering process, will take care of the overall energy balance. In the forward direction, the calculated energy loss due to scattering is twice the reflected energy, but half the energy loss is the scattered energy in the forward direction, which is treated as energy gain in that direction, so the net energy loss

net loss = total scattered energy – energy being scattered in (gain)

is exactly the amount of the back reflected energy. Therefore the energy conservation law is observed in the radiative transfer treatment.